21st Australasian Fluid Mechanics Conference
Adelaide, Australia
10–13 December 2018

Impulsively Generated Incompressible Two-Phase Flow and the Asai Thermal Ink-jet Model

G. D. McBain[1] **and S. G. Mallinson**[1,2]

[1]Modelling & Simulation, Memjet North Ryde Pty Ltd
Macquarie Park, New South Wales 2113, Australia

[2]School of Mechanical & Manufacturing Engineering, The University of New South Wales
Kensington, New South Wales 2052, Australia

Abstract

A widespread model of thermal ink-jet actuation prescribes the pressure of the expanding bubble as a rapidly decreasing function of time, this being taken as a finite version of a Dirac impulse with only the integral with respect to time mattering. Here it is shown that the impulse is actually easier to treat numerically than the bounded approximation and an implementation in OpenFOAM is described; however, solutions so obtained reveal that the flow does depend on the timescale over which the pressure is applied, i.e. on first and higher moments of the pressure function. An asymptotic expansion of a lumped linear model is derived which predicts the dependence of the induced flow on these moments for an arbitrarily shaped pressure pulse.

Introduction

A thermal ink-jet is a device for ejecting microscopic droplets, e.g. for printing [3, 29]. As sketched in figure 1, it is a vessel filled with ink, open at one end through a nozzle to the air and at the other to a reservoir. It contains a heater which suddenly boils ink near it so that the expanding bubble pushes ink forwards out through the nozzle. Following the nucleation of the bubble, the flow consists of three distinct phases: the vapour bubble, the liquid ink, and the ambient air. The ink and air are essentially incompressible but the overall dynamics is complicated by strong interaction between the thermodynamics of the bubble and its heat, mass, and momentum transfer with the ink.

To alleviate the complexity of the bubble, a much simpler decoupled model was introduced [3] in which it is replaced with a pressure which is a prescribed function of time; we also mention a number of precursors [6, 17, 13, 11]. Although more recent computational models have been developed which include a coupled bubble [10, 29, 23, 24, 30, 25], the uncoupled model continues to usefully simulate aspects of ink-jet actuation [12, 9, 28, 20, 14, 15, 16].

Asai has written much on ink-jet technology [4, 5, 1, 2]; here 'the Asai model' is merely used as a concise name for the 'Method of Calculation' [3], and more specifically for modelling the bubble by a prescribed history of pressure. Originally it was suggested that 'the bubble pressure can be modeled by an impulsive function' [3], and this had been done in an earlier lumped model [2], but then recourse to generalized functions was avoided by arguing that 'numerically, such impulsive pressure change can be described by a rapidly decreasing function of time' [3] with the same *pressure impulse* (integral of pressure over time). While this is asymptotically true, the first purpose of the present paper is to show that actually the direct use of an impulsive pressure is by no means difficult.

The second purpose is to see whether the actuating pressure can indeed be characterized purely in terms of its impulse [11] or its timing is significant [17]; i.e. how slow the pressure has to be before its higher moments with respect to time become relevant.

The Asai Ink-Jet Model

The method presented here differs from the original 'Method of Calculation' [3] in which the equations of motion were only solved in the ink with a constant pressure imposed beyond the meniscus outside the nozzle and a varying pressure in the bubble. These days, it is more usual to fill out the domain with a second immiscible incompressible air-like fluid outside the nozzle and inside the bubble using the 'one-fluid formulation' [7, 27] with density $\rho = \rho(\alpha)$ and viscosity $\mu = \mu(\alpha)$ being functions of the volume-of-fluid α interpolating between the values for air and water at $\alpha = 0$ and 1, respectively. The surface tension, previously part of the boundary condition on the interface, is represented by a continuous volumetric force [8] . The essential feature of the model remains the prescription of the pressure in the bubble; here this is shifted from the interface to the surface of the actuator inside the bubble.

Governing Equations

The system for the evolution of the velocity $\mathbf{u}$ in time t is thus

$$\rho\frac{\mathrm{D}\mathbf{u}}{\mathrm{D}t} = \rho\mathbf{F} - \nabla p + \nabla\cdot\left\{\mu\left(\nabla\mathbf{u} + [\nabla\mathbf{u}]^{\mathrm{T}}\right)\right\} \tag{1}$$

$$\nabla\cdot\mathbf{u} = 0 \tag{2}$$

$$\frac{\mathrm{D}\alpha}{\mathrm{D}t} = 0, \tag{3}$$

where $\mathbf{F}$ includes capillarity.

In the model, the pressure p is prescribed far off in the air as atmospheric, at the upstream ink reservoir as some other constant, and at the surface of the heater as a rapidly decreasing function of time such as [2, 3]

$$p(t) = p_0 \mathrm{e}^{-(t/t_0)^\lambda} \tag{4}$$

plus a slower varying more bounded part which is of less interest here. Where the velocity crosses the boundary into the domain, a value for α is prescribed; $\alpha = 0$ for the heater. On the other walls, $\mathbf{u} = \mathbf{0}$ and a contact angle is set.

This is a standard set of equations and canned solvers are available; here `interFoam` from the free OpenFOAM suite was used in figure 2 to repeat Asai's [3] case $\lambda = \frac{1}{2}$, $t_0 = 0.17\,\mu\mathrm{s}$.

Impulsively Generated Flow

The form of the pressure equation (4) is a bounded approximation to a Dirac δ function, approaching $\Pi\delta(t)$ as $t_0 \to 0$ with λ fixed and p_0 varying inversely with t_0 so that the pressure impulse $\Pi \equiv m_0$ is constant, where m_k is the k-th moment:

$$m_k \equiv \int_0^\infty t^k p(t)\,\mathrm{d}t. \tag{5}$$

In the Navier–Stokes equation (1), if the energy and therefore velocity is to remain finite, a Dirac pressure spike can only be

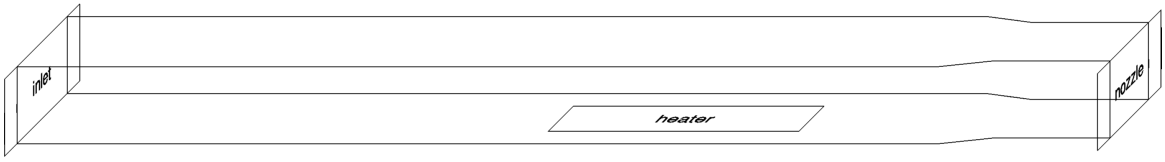

Figure 1: Sketch of Asai's [3] 'prototype bubble jet printer'. It is filled with ink from to the left of the inlet through to the nozzle, to the right of which is air. The top of the heater is 30 µm × 150 µm.

Figure 2: Elevation in the plane of left–right symmetry showing ink (grey) and airy 'bubble' (white) after 30 µs, simulated with `interFoam`; cf. [3, figure 3]

balanced by the temporal derivative of the velocity with the latter having a Heaviside step [18]; thus asymptotically,

$$\rho \frac{\partial \{\mathbf{u}\mathrm{H}(t)\}}{\partial t} = -\nabla \{\Pi \delta(t)\} \tag{6}$$

or

$$\mathbf{u} = -\rho^{-1} \nabla \Pi. \tag{7}$$

An equation for the pressure impulse field Π is obtained by substituting equation (7) for the impulsive velocity into the continuity equation (2):

$$-\nabla \cdot \left(\rho^{-1} \nabla \Pi\right) = 0. \tag{8}$$

Impulsively Generated Flow in Inhomogeneous Fluid

For a single homogeneous fluid, ρ can be taken outside the divergence in equation (8) and the pressure impulse satisfies Laplace's equation [18]; for inhomogeneous fluid, it must be retained as a spatially varying coefficient.

Equation (8) was previously derived for the impulsive pressure in a stratified fluid [22]. It also arose in another discussion of computational multiphase flow in trying to filter out the non-solenoidal component of an initial condition [7].

Laplace's equation would suffice for a post-impulse nonzero initial condition for the velocity in Asai's [3] liquid-only simulation, but if the air is to be included as well, as it must be with one-fluid solvers like `interFoam`, the density must be retained as a spatially varying coefficient. Although the physical effect of the air on the ink is indeed essentially limited to its pressure, difficulties will arise if the initial condition on velocity does not satisfy the continuity equation (2) [7].

Solving for the Impulsively Generated Flow in OpenFOAM

While none of the standard OpenFOAM solvers can solve equation (8), little had to be done to generalize `potentialFoam`; indeed, only one line in the main C++ source file was modified, to include the varying coefficient of equation (8):

```
fvm::laplacian(1.0/rho, Phi)
```

although other subsidiary files had to be included from `interFoam` in order to set up the spatially varying `rho`.

The Two Approaches to Initial Impulses

The concept of having two equivalent sets of initial conditions, before and after an impulse, is common in electrical circuit analysis [19, pp. 470–480]. Mechanically, consider golf: one might contrast, on the one hand, simulating a club hitting a ball, the contact problem and elastic deformation, with, on the other, the comparatively simple ballistics of the rigid ball after it has received its momentum. Similarly in the bubble jet, it is easier to compute the impulsively generated velocity field by solving the potential-like equation (8) than to resolve in time the rapidly varying pressure of equation (4) and the correspondingly rapid acceleration of ink and air.

The Complex Lamellar Impulsively Generated Flow

Whereas flow impulsively generated in a uniform fluid is potential, equation (7), being the product of one scalar and the gradient of another is *complex lamellar* [26]. Thus it is not necessarily irrotational. The vorticity is $\nabla \times \mathbf{u} = -\nabla(1/\rho) \times \nabla\Pi$; the impulse might set up a vortex sheet at an interface across which the density jumps. A couple of one-dimensional examples might be instructive. First consider two fluids in series: the impulsive pressure drops in proportion to the density and they set off with the same velocity, the whole being irrotational since the impulsive pressure gradient is normal to the interface. Second, two in parallel: the impulsive pressure drops are the same but the imparted velocities are inversely proportional to the density, with a vortex sheet along the interface.

Application to Modeling Ink-Jets

With a solver for equation (8) in hand, simulating Asai's prototype bubble jet becomes simpler: the preliminary solution provides the initial condition for velocity and the part of the pressure imposed on the heater corresponding to the impulse is omitted. Qualitatively the overall results are similar, but a closer quantitative examination in figure 3 using the flow-rate through the heater (as done by Deshpande [12, figures 3, 5, 7]) reveals that the flow-rate for Asai's pressure equation (4) with $t_0 = 0.17\,\mu\text{s}$ is not the same as that generated impulsively; however, the theory is asymptotically validated, being approached as the pressure is delivered more rapidly ($t_0 \to 0$).

The pure impulse ($t_0 = 0$) provides a nonzero velocity at $t = 0$ and therefore a jump in flow-rate. The ratio of Π to this jump is defined as the *inertance* L. If the flow-rate in figure 3 is fitted to the log–linear form

$$q(t) \sim \frac{\Pi}{L} \mathrm{e}^{-Rt/L}, \tag{9}$$

the quantity R has the dimensions of hydraulic resistance and $L/R \approx 6\,\mu\text{s}$ is a hydraulic timescale.

This might seem long compared to the 0.17 µs proposed for t_0 [3] but unless $\lambda = 1$ in equation 4, t_0 is a misleading indicator of the timescale of the pressure input. A more physical value might be based on the ratio of the first two moments from equation (5); for equation (4) with $\lambda = \frac{1}{2}$, this is $m_1/m_0 = 6t_0 \approx 1\,\mu\text{s}$.

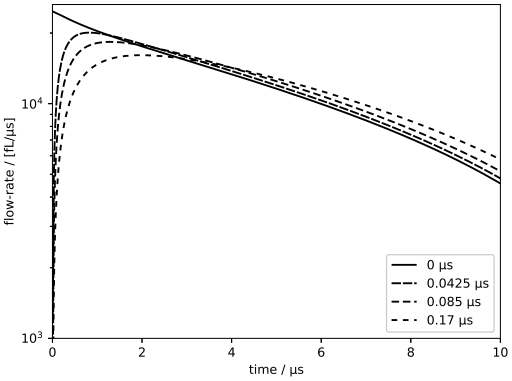

Figure 3: Bubble expansion, with the same pressure impulse applied (*solid*) instantaneously, solving equations (2) and (7) for the initial velocity and (*dashed*) over time by equation (4)

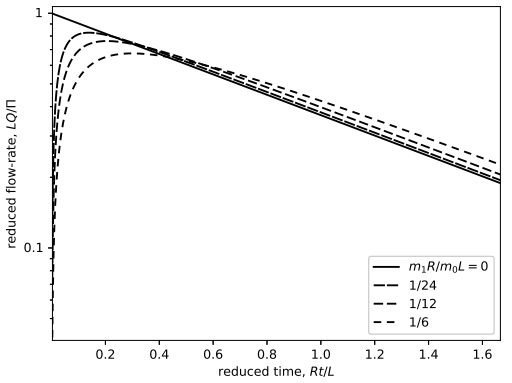

Figure 4: Flow-rate from equation (11) in the linear lumped model with pressure from (4) and ratios of timescales m_1R/m_0L chosen to roughly match figure 3

Impulsive and Phased Pressure

A Lumped Model

Equation (9) solves the lumped hydraulic equation [12]

$$L\dot{q} + Rq = p(t) \tag{10}$$

with impulsive $p(t) = \Pi\delta(t)$ and $q(0) = 0$. For arbitrary $p(t)$:

$$q(t) = L^{-1}\int_0^t \mathrm{e}^{R(t'-t)/L} p(t')\,\mathrm{d}t'. \tag{11}$$

This is plotted in figure 4 with pressure equation (4) for values of the ratio of timescales $(L/R)/(m_1/m_0)$ roughly corresponding to those of figure 3.

As the lumped equation (11) qualitatively reproduces the full multiphase three-dimensional dynamics of figure 3, it is used to investigate the failure of the hypothesis that only the zeroth moment of $p(t)$ matters at times long after the pressure input has subsided—as seen there, the flow-rate after the passing of the pressure is a quarter higher than that due to impulse alone.

Asymptotic Expansion

Rewriting equation (11) with $p(t) = p_0 f(t/t_0)$ where t_0 is a characteristic timescale for the pressure as in equation (4),

$$q(t) = \frac{p_0}{R}\mathrm{e}^{-Rt/L}\int_0^{Rt/L} \mathrm{e}^{\tau} f\left(\frac{L}{Rt_0}\tau\right)\mathrm{d}\tau, \tag{12}$$

an asymptotic expansion for $t_0 \ll L/R$ can be obtained by repeated integration by parts:

$$\mathrm{q}(t) \sim \frac{p_0 t_0}{L}\sum_{k=0}^{\infty}\left(\frac{Rt_0}{L}\right)^k \left\{\mathrm{e}^{-Rt/L}\mathrm{i}^{k+1}f(0) - \mathrm{i}^{k+1}f\left(\frac{t}{t_0}\right)\right\} \tag{13}$$

where $\mathrm{i}^0 f \equiv f$ and for $k = 1, 2, \ldots$ the iterated integrals are

$$\mathrm{i}^k f(\theta) \equiv \int_\theta^\infty \mathrm{i}^{k-1} f(\theta)\,\mathrm{d}\theta. \tag{14}$$

The final decay of the flow-rate is

$$q(t) \sim \frac{p_0 t_0}{R}\mathrm{e}^{-Rt/L}\sum_{k=0}^{\infty}\left(\frac{Rt_0}{L}\right)^k \mathrm{i}^{k+1}f(0). \tag{15}$$

From Cauchy's formula for iterated integrals [21, p. 5]:

$$k! p_0 \mathrm{i}^{k+1} f(0) = p_0\int_0^\infty \theta^k f(\theta)\,\mathrm{d}\theta \equiv \frac{m_k}{t_0^{k+1}} \tag{16}$$

so that

$$q(t) \sim \frac{\Pi}{L}\mathrm{e}^{-Rt/L}\sum_{k=0}^{\infty}\frac{M_k}{k!}\left(\frac{Rm_1}{Lm_0}\right)^k, \tag{17}$$

where the dimensionless small parameter Rm_1/Lm_0 of the asymptotic expansion is the ratio of the pressure and hydraulic timescales and the moments are normalized as

$$M_k \equiv \frac{m_k/m_0}{(m_1/m_0)^k}. \tag{18}$$

Equation (17) shows that the higher temporal moments of the pressure input increase the later flow-rate relative to the impulsively driven equation (9), exactly as seen in figures 3 and 4.

For Asai's λ pressure equation (4)

$$M_k = \frac{\Gamma\left(\frac{k+1}{\lambda}\right)}{\Gamma\left(\frac{1}{\lambda}\right)}\left\{\frac{\Gamma\left(\frac{1}{\lambda}\right)}{\Gamma\left(\frac{2}{\lambda}\right)}\right\}^k. \tag{19}$$

With this, equation (17) is compared with the `interFoam` simulations of figure 3 at 10 μs in figure 5.

Conclusions

The impulsively generated incompressible multiphase flow can be computed by solving a Laplace equation with variable coefficient. This can be used to drive Asai's thermal ink-jet model without having to approximate the Dirac-δ pressure impulse with a bounded drawn-out function; however, it turns out that these finite pressure functions introduced for supposed numerical convenience are not separated in timescale from the hydraulics of typical devices. The flow does approach the impulsively generated one as the pressure-time tends to zero but for typical finite durations, there is an enduring effect. This can be explained in terms of a linear first-order inertance–resistance response which shows how the higher moments of the pressure pulse with respect to time affect the later flow.

Acknowledgements

We thank Dr Paul Croaker of ESI Pacific for much assistance with a previous effort at this problem and Dr Darrin Stephens of Applied CCM for expert advice in programming OpenFOAM.

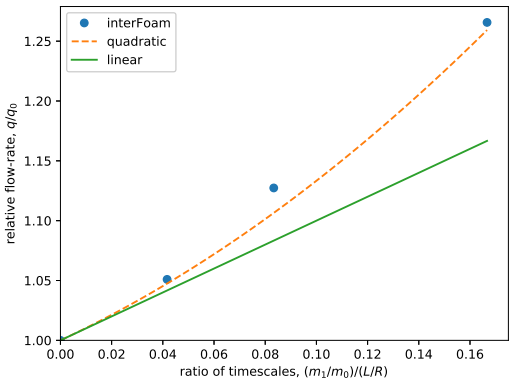

Figure 5: Excess of flow-rate at 10 µs driven by finite pressure pulse relative to impulsively driven value; comparison with the first three terms of the asymptotic equation (17)

References

[1] Asai, A., Application of the nucleation theory to the design of bubble jet printers, *Jap. J. Appl. Phys.*, **28**, 1989, 909–915.

[2] Asai, A., Bubble dynamics in boiling under high heat flux pulse heating, *J. Heat Transfer*, **113**, 1991, 973–979.

[3] Asai, A., Three-dimensional calculation of bubble growth and drop ejection in a bubble jet printer, *J. Fluids Eng.*, **114**, 1992, 638–641.

[4] Asai, A., Hara, T. and Endo, I., One-dimensional model of bubble growth and liquid flow in bubble jet printers, *Jap. J. Appl. Phys.*, **26**, 1987, 1794–1801.

[5] Asai, A., Hirasawa, S. and Endo, I., Bubble generation mechanism in the bubble jet recording process, *J. Imaging Tech.*, **14**, 1988, 120–124.

[6] Beasley, J. D., Model for fluid ejection and refill in an impulse drive jet, *Photo. Sci. & Eng.*, **21**, 1977, 78–82.

[7] Bierbrauer, F. and Zhu, S. P., A solenoidal initial condition for the numerical solution of the Navier–Stokes equations for two-phase incompressible flow, *Comp. Mod. Eng. Sci.*, **19**, 2007, 1–22.

[8] Brackbill, J. U., Kothe, D. B. and Zemach, C., A continuum method for modeling surface tension, *J. Comp. Phys.*, **100**, 1992, 335–354.

[9] Chen, P.-H., Chen, W.-C. and Chang, S. H., Bubble growth and ink ejection process of a thermal ink jet printhead, *Int. J. Mech. Sci.*, **39**, 1997, 683–695.

[10] Cornell, R., Nucleation quality and bubble momentum and their effect on droplet velocity and stability, in *Recent Progress in Ink Jet Technologies II*, editor E. Hanson, 1999, 33–38.

[11] Deshpande, N. V., Fluid mechanics of bubble growth and collapse in a thermal ink jet printhead, in *SPIE Proceedings*, 1989, 273–289.

[12] Deshpande, N. V., Significance of inertia and resistance in fluidics of thermal ink-jet transducers, *J. Imaging Sci. & Tech.*, **40**, 1996, 396–400.

[13] Fromm, J., A numerical study of drop-on-demand ink jets, in *Proceedings of the Second International Colloquium on Drops and Bubbles*, editor D. H. Lecroissette, 1982, 54–62.

[14] Glatzel, T., Litterst, C., Cupelli, C., Lindemann, T., Moosmann, C., Niekrawietz, R., Streule, W., Zengerle, R. and Koltay, P., Computational fluid dynamics (CFD) software tools for microfluidic applications—a case study, *Computers & Fluids*, **37**, 2008, 218–235.

[15] He, B., Yang, S., Qin, Z., Wen, B. and Zhang, C., The roles of wettability and surface tension in droplet formation during inkjet printing, *Sci. Rep.*, **7**.

[16] Jiang, H. and Tan, H., One dimensional model for droplet ejection process in inkjet devices, *Fluids*, **3**, 2018, 28.

[17] Kyser, E. L., Collins, L. F. and Herbert, N., Design of an impulse ink jet, *J. Appl. Photo. Eng.*, **7**, 1981, 73–79.

[18] Lamb, H., *Hydrodynamics*, Cambridge University Press, 1932, 6th edition.

[19] Ley, J. B., Lutz, S. G. and Rehberg, C. F., *Linear Circuit Analysis*, McGraw-Hill, 1959.

[20] Lindemann, T., *Droplet Generation From the Nanoliter to the Femtoliter Range*, Ph.D. thesis, Albert-Ludwigs-Universität, 2006.

[21] Lovitt, W. V., *Linear Integral Equations*, Dover, 1950.

[22] Saffman, P. G. and Meiron, D. I., Kinetic energy generated by the incompressible Richtmyer–Meshkov instability in a continuously stratified fluid, *Phys. Fluids A*, **1**, 1989, 1767–1771.

[23] Sen, A. K. and Darabi, J., Droplet ejection performance of a monolithic thermal inkjet print head, *J. Micromech. Microeng.*, **17**, 2007, 1420–1427.

[24] Suh, Y. and Son, G., A level-set method for simulation of a thermal inkjet process, *Num. Heat Transfer B: Fund.*, **54**, 2008, 138–156.

[25] Tan, H., An adaptive mesh refinement based flow simulation for free-surfaces in thermal inkjet technology, *Int. J. Multiphase Flow*, **82**, 2016, 1–16.

[26] Thomson, W., A mathematical theory of magnetism—continuation of part I, *Phil. Trans. R. Soc. London*, **141**, 1851, 269–285.

[27] Tryggvason, G., Scardovelli, R. and Zaleski, S., *Direct Numerical Simulation of Gas–Liquid Multiphase Flows*, Cambridge University Press, 2011.

[28] Wu, H.-C., Hwang, W.-S. and Lin, H.-J., Development of a three-dimensional simulation system for micro-inkjet and its experimental verification, *Mat. Sci. & Eng. A*, **373**, 2004, 268–278.

[29] Zhao, Z., Glod, S. and Poulikakos, D., Pressure and power generation during explosive vaporization on a thin-film microheater, *Int. J. Heat Mass Transfer*, **43**, 2000, 281–296.

[30] Zhou, H. and Gué, A. M., Simulation model and droplet ejection performance of a thermal-bubble microejector, *Sensors & Actuators B: Chem.*, **145**, 2010, 311–319.